PHYSICAL REVIEW E **68**, 031501 (2003)

# Difference and similarity of dielectric relaxation processes among polyols

Ayumi Minoguchi, Kei Kitai, and Ryusuke Nozaki
*Division of Physics, Graduate School of Science, Hokkaido University, Sapporo 060-0810, Japan*

(Received 27 December 2002; revised manuscript received 25 March 2003; published 5 September 2003)

Complex permittivity measurements were performed on sorbitol, xylitol, and sorbitol-xylitol mixture in the supercooled liquid state in an extremely wide frequency range from 10 $\mu$Hz to 500 MHz at temperatures near and above the glass transition temperature. We determined detailed behavior of the relaxation parameters such as relaxation frequency and broadening against temperature not only for the $\alpha$ process but also for the $\beta$ process above the glass transition temperature, to the best of our knowledge, for the first time. Since supercooled liquids are in the quasi-equilibrium state, the behavior of all the relaxation parameters for the $\beta$ process can be compared among the polyols as well as those for the $\alpha$ process. The relaxation frequencies of the $\alpha$ processes follow the Vogel-Fulcher-Tammann manner and the loci in the Arrhenius diagram are different corresponding to the difference of the glass transition temperatures. On the other hand, the relaxation frequencies of the $\beta$ processes, which are often called as the Johari-Goldstein processes, follow the Arrhenius-type temperature dependence. The relaxation parameters for the $\beta$ process are quite similar among the polyols at temperatures below the $\alpha\beta$ merging temperature, $T_M$. However, they show anomalous behavior near $T_M$, which depends on the molecular size of materials. These results suggest that the origin of the $\beta$ process is essentially the same among the polyols.

DOI: 10.1103/PhysRevE.68.031501 PACS number(s): 64.70.Pf, 61.25.Em, 77.22.Gm

## I. INTRODUCTION

There are two dielectric relaxation processes in many supercooled glass formers, i.e., the primary $\alpha$ relaxation process and the secondary $\beta$ relaxation process. The $\alpha$ process shows non-Arrhenius-type temperature dependence described by Vogel-Fulcher-Tammann (VFT) function [1–3],

$$\langle \tau \rangle = \tau_{VFT} \exp\left( \frac{B_{VFT}}{T - T_0} \right), \tag{1}$$

where $\langle \tau \rangle$ is the mean relaxation time, $\tau_{VFT}$ represents the relaxation time at $T \to \infty$, $T_0$ is the VFT temperature where the mean relaxation time diverges and $B_{VFT}$ is connected to the strength parameter, which is related to the fragility [39]. It is considered that the $\alpha$ process is the structural relaxation process and closely connected to glass transition phenomena. Recently, one has been trying to understand the $\alpha$ process using a concept of "cooperative molecular motion" and there are several theories or models [4–10].

On the other hand, secondary $\beta$ process (so-called the Johari-Goldstein process [12]) is observed in many glass formers at higher-frequency side of the $\alpha$ process. The $\beta$ process obeys the Arrhenius-type temperature dependence given by

$$\langle \tau \rangle = \tau_A \exp\left( \frac{E_A}{RT} \right), \tag{2}$$

where $\langle \tau \rangle$ is the mean relaxation time, $\tau_A$ represents the relaxation time at $T \to \infty$, and $E_A$ is the activation energy. It has been considered that the $\beta$ process is connected to local molecular motions, in contrast with the $\alpha$ process. It is also considered that the $\beta$ process is concerned with the essentiality of amorphous matters, such as the supercooled liquids and the glassy solids, because the $\beta$ process is observed not only in the supercooled liquid state but also in the glassy state. Although several understandings have been examined [9–11,13,14], the mechanism of the $\beta$ processes is still unclear.

While these two processes are observed separately at lower temperatures above the glass transition temperature, they approach each other with increasing temperature and merge together at a higher temperature $T_M$. There would be a kind of strong correlation between the $\alpha$ and the $\beta$ processes at near the merging temperature $T_M$, which sometimes cannot be determined precisely. It must be very important to study the relation between the behavior of the $\alpha$ process and the appearance of the $\beta$ process to understand the glass transition phenomena in detail.

The merging of the $\alpha$ and $\beta$ processes is classified into two scenarios by Donth *et al.* [15,16]. Scenario I shows a continuity of the relaxation frequency of the $\beta$ process below $T_M$ and the relaxation frequency of the process above $T_M$ with a bend in the Arrhenius diagram. The $\alpha$ process appears at around $T_M$. The values of the relaxation strength of the $\alpha$ and $\beta$ processes have the same order of magnitude. Scenario II shows a quasicontinuity of the relaxation frequency of the $\alpha$ process below $T_M$ and the relaxation frequency of the process above $T_M$ in the Arrhenius diagram. The value of the relaxation strength of the $\beta$ process is smaller than that of the $\alpha$ process.

However, some glass formers do not show the $\beta$ process clearly, but an excess wing, which is the high-frequency wing of the $\alpha$ process, is observed. It is proposed that glass formers are divided into two classes: type *A* with an excess wing and type *B* with a $\beta$ process [17]. Many glass formers are classified into type *B*. Glycerol [$CH_2OH(CHOH)CH_2OH$] and propylene carbonate are well-known glass formers classified into type *A* [17,19,20].

Sorbitol [$CH_2OH(CHOH)_4CH_2OH$] and xylitol [$CH_2OH(CHOH)_3CH_2OH$] are typical glass-forming liquids and belong to a series of polyols [21–28]. Molecules form the intermolecular hydrogen-bonding network. In supercooled sorbitol and xylitol, two dielectric relaxation processes, the $\alpha$ and $\beta$ processes, exist [21,29]. The $\beta$ process in sorbitol has relatively large relaxation strength for the simple associated liquid. So this system is suitable to study relation between the $\alpha$ and the $\beta$ processes. From our complex permittivity measurements, sorbitol and xylitol are classified into scenario II and type *B*. It is noted that glycerol also belongs to a series of polyols, however, does not show the $\beta$ process.

In the present work, we made broadband complex permittivity measurements of sorbitol, xylitol, and sorbitol-xylitol mixture in the supercooled liquid state at temperatures near and above the glass transition temperature $T_g$. It must be very important to examine such a broadband dielectric behavior of supercooled polyols to understand the mechanism of the $\alpha$ and $\beta$ processes. The behavior of all the relaxation parameters not only for the $\alpha$ process but also for the $\beta$ process can be compared among the polyols because supercooled liquids are in the quasiequilibrium state. Studying the mixture in addition to pure constituents would be quite helpful. We suggest the origins of the $\alpha$ and $\beta$ processes in polyols from the microscopic viewpoint and try to understand the curious behavior of glycerol.

## II. EXPERIMENT

Crystal powders of sorbitol and xylitol was purchased from Kishida Chemical. The melting temperatures $T_m$ obtained by differential scanning colorimetry (DSC) measurements of sorbitol and xylitol are 368 K and 366 K, respectively [30]. To remove the moisture, the samples of powder were dried in a vacuum chamber at room temperature. In the case of pure sorbitol and xylitol, the samples of powder were annealed at temperature near $T_m$ for 24 h in a vacuum chamber. In the case of sorbitol-xylitol mixture, dried powders of sorbitol and xylitol were mixed (the molar ratio is 1:1). The mixed powder was annealed at temperature near $T_m$ of sorbitol for 24 h in a vacuum chamber. The liquid sorbitol, xylitol, and the mixture were quenched to the temperature for the measurement in the dielectric cell.

The dielectric measurements were made in the frequency range from 10 $\mu$Hz to 500 MHz. In order to cover the wide frequency range, four different measuring systems were used. From 10 $\mu$Hz to 0.3 Hz, a time-domain spectrometer was employed which has been developed by us. A steplike voltage, which is produced by computer (NEC PC9801As) with a digital-analog converter and a high-speed power amplifier (NF2010), is applied to a three-terminal parallel-plate capacitor filled with the sample. Corresponding charging and discharging currents were measured by an electrometer (KEITHLEY 6521). The complex permittivity is obtained from the Fourier transform of the voltage and the current data with time. From 0.1 Hz to 100 Hz, a fast Fourier transform analyzer (HP35670A) and a current amplifier (KEITHLEY 428) were employed using the same parallel-plate sample cell. We used a LCR meter (HP4284A) and the same parallel-plate sample cell as a four-terminal circuit between 20 Hz and 1 MHz. From 1 MHz to 500 MHz, a network analyzer (HP4195A) was used with the transmission line method. A coaxial sample cell is located at the end of a coaxial line. The values of the complex permittivity were obtained from reflection measurements. Below 1 MHz, the cryostat with the sample cell is set in a bath filled with mixture of water and ethylene glycol. Temperature of the cell was controlled within 0.05 K. Above 1 MHz, the temperature of the sample cell inserted into water jacket was controlled within 0.1 K.

The complex permittivity measurements were performed at temperature ranges between 263 K and 346 K for sorbitol, 250 K and 346 K for xylitol and 253 K and 344 K for the mixture.

## III. RESULTS AND DISCUSSION

Dielectric losses of sorbitol, sorbitol-xylitol mixture, and xylitol at various temperatures are shown in Figs. 1(a)–1(c), respectively. The $\alpha$ and $\beta$ processes are observed clearly at lower temperature. As the temperature increases, the $\alpha$ relaxation peak comes closer to the $\beta$ relaxation peak and then these two processes merge into only one process. It should be pointed out that any other process except for the $\alpha$ and $\beta$ processes is not observed even for the mixture.

The complex permittivity of sorbitol, xylitol, and the mixture can be described by using the sum of the Havriliak-Negami function [31] for the $\alpha$ process and the Cole-Cole function [32] for the $\beta$ process as has been reported for many other systems [21,29]. Thus, the fitting function is given by

$$\varepsilon^*(\omega)=\varepsilon_\infty+\frac{\Delta\varepsilon^{\alpha}}{[1+(i\omega\tau_{HN}^{\alpha})^{\delta^{\alpha}}]^{\gamma^{\alpha}}}+\frac{\Delta\varepsilon^{\beta}}{1+(i\omega\tau_{CC}^{\beta})^{\delta^{\beta}}}, \quad (3)$$

where supersuffixes $\alpha$ and $\beta$ represent the $\alpha$ and the $\beta$ processes, respectively. Parameter $\Delta\varepsilon$ is the relaxation strength, $\tau$ is the relaxation time, and $\gamma$ and $\delta$ are shape parameters which represent asymmetric and symmetric broadenings, respectively. $\varepsilon_\infty$ is the high-frequency limiting permittivity and $\omega$ is an angular frequency. Solid curves obtained from Eq. (3) are also shown in Fig. 1. The experimental data are described well by Eq. (3).

Figure 2 shows plots of frequency dependence of dielectric loss of sorbitol at 283 K, xylitol at 263 K, and sorbitol-xylitol mixture at 272 K. These data are chosen to survey differences in appearance of the $\alpha$ and $\beta$ processes among the different materials. It is clear that all the loci indicate the $\alpha$ process with larger dielectric loss and the $\beta$ process with smaller loss at high-frequency side of the $\alpha$ process. It is noted that the loss intensity depends on the size of molecule. The loss intensity for the $\alpha$ process of sorbitol is smaller than that of xylitol, and that of the mixture is intermediate between those of sorbitol and xylitol. On the other hand, the tendency for the $\beta$ process is in opposite direction to that for the $\alpha$ process. All these are consistent with those reported for several pure materials [21,29].

Figures 3 and 4(a) show the Arrhenius diagrams for all the materials. These Arrhenius diagrams are the plots of the relaxation frequency $f_m$ against the reciprocal temperature. $f_m$

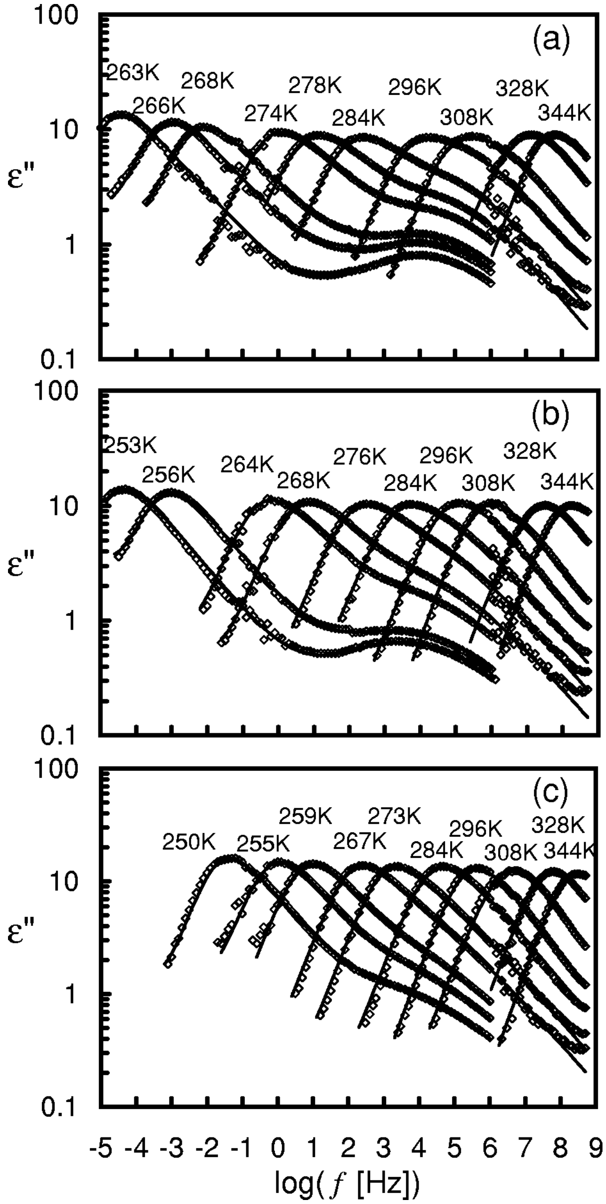

FIG. 1. Dielectric losses of sorbitol (a), sorbitol-xylitol mixture (b), and xylitol (c) at various temperatures. Solid curves are the fitting function described by Eq. (3).

is the frequency with maximum dielectric loss for the corresponding fitting function being used in Eq. (3). We use $f_m$ instead of the relaxation time, such as $\tau_{HN}$ and $\tau_{CC}$, because $f_m$ does not depend on the choice of fitting function. There is a relation $f_m = 1/2\pi\langle\tau\rangle$. The relaxation frequency of the $\alpha$ process, $f_m^\alpha$, for all the materials follows the VFT manner described by

$$\log_{10} f_m = A - \frac{B}{T - T_0}, \tag{4}$$

where $A = \log_{10}(1/2\pi\tau_{VFT})$, $B = B_{VFT}/2.303$, and $T_0$ is the VFT temperature. $A$ represents the attempt frequency at $T \rightarrow \infty$. On the other hand, the relaxation frequency of the $\beta$ process, $f_m^\beta$, for all the materials follows the Arrhenius manner described by

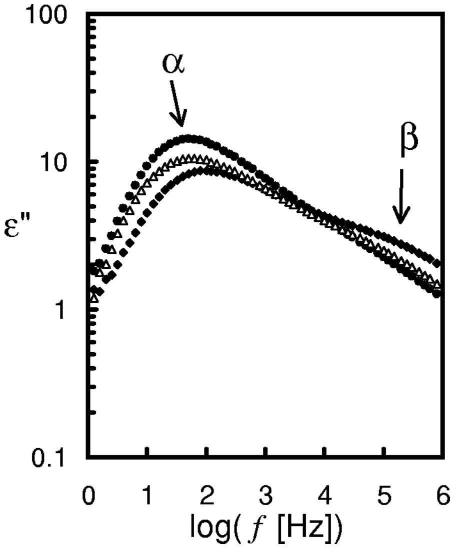

FIG. 2. Dielectric losses of sorbitol at 282 K (solid diamond), xylitol at 263 K (solid circle), and mixture at 272 K (open triangle).

$$\log_{10} f_m = C - \frac{E_A}{2.303RT}, \tag{5}$$

where $C = \log_{10}(1/2\pi\tau_A)$ and $E_A$ is the activation energy. $C$ represents the attempt frequency at $T \rightarrow \infty$.

The temperature dependence of $f_m^\alpha$ in various glass formers cannot be described precisely by using only one VFT function. It has been reported that two VFT functions are required to describe the temperature dependence of $f_m^\alpha$ for some systems [33–35]. We have reported that the $\alpha$ process in sorbitol at temperatures near the glass transition temperature $T_g^*$, which is the temperature with 0.01 Hz of $f_m^\alpha$, cannot be described using only one VFT function determined using data at higher temperatures [21]. Especially, in the case that the relaxation strength of the $\beta$ process, $\Delta\varepsilon^\beta$, is relatively large, the behavior of the $\alpha$ and $\beta$ processes near $T_M$ cannot be distinguished clearly due to the strong correlation between the two processes. To discuss the behavior of the loci for the $\alpha$ process in the Arrhenius diagram is not the aim of this paper. Therefore, in this work, VFT curves are determined using data below $T_M$ just to compare the behavior of the $\alpha$ processes among the materials.

As shown in Fig. 4(a), the curves of the VFT functions for all the materials are different corresponding to the difference of $T_g^*$. $T_g^*$ of sorbitol and xylitol are 268 K [21] and 248 K, respectively. $T_g$ of sorbitol and xylitol obtained by DSC measurement are 267 K and 249 K, respectively [30]. $T_g^*$ of the mixture is 258 K, which is intermediate value between those of sorbitol and xylitol. The fragility index $m$ was given to be 101 for sorbitol, 86 for xylitol, and 93 for the mixture, respectively.

On the other hand, the $\beta$ processes in sorbitol, xylitol, and the mixture show the Arrhenius-type temperature depen-

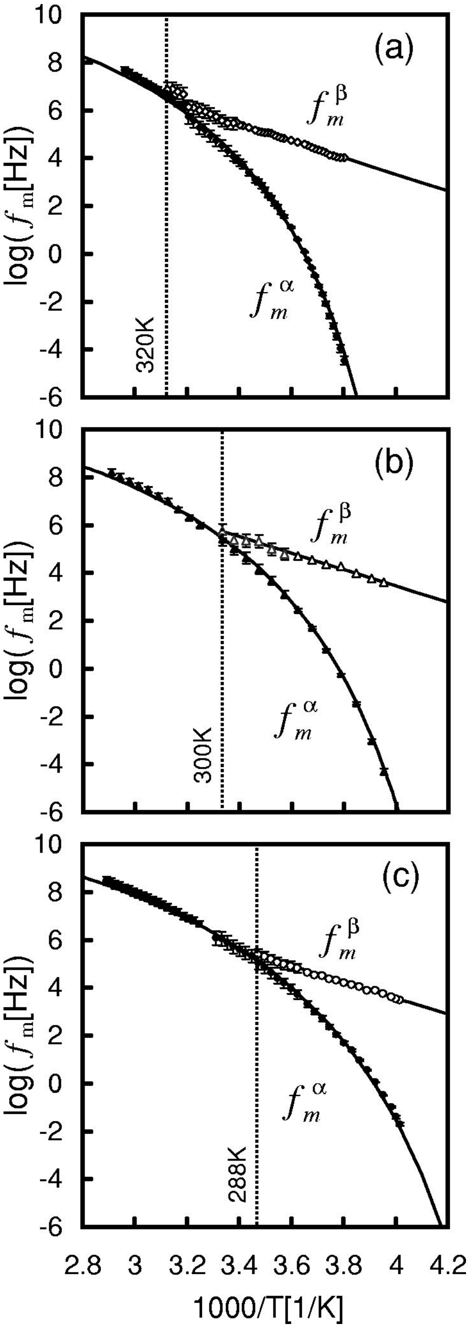

FIG. 3. Arrhenius diagrams of sorbitol (a), mixture (b), and xylitol (c). Dotted lines represent $T_M$ of sorbitol (320 K), mixture (300 K), and xylitol (288 K), respectively. (a) Solid and open diamonds represent $f_m^\alpha$ and $f_m^\beta$ for sorbitol, (b) solid and open triangles represent $f_m^\alpha$ and $f_m^\beta$ for mixture, and (c) solid and open circles represent $f_m^\alpha$ and $f_m^\beta$ for xylitol. Solid curves were obtained from Eq. (4) (sorbitol: $A=12.7$, $B=572$ K, and $T_0=229$ K, xylitol: $A=12.85$, $B=640$ K, and $T_0=205$ K, mixture: $A=12.77$, $B=606$ K, and $T_0=217$ K). Solid lines were obtained from Eq. (5) [sorbitol: $C=17.2$ and $E_A=80$ (kJ/mol), xylitol: $C=17.12$ and $E_A=78$ (kJ/mol), sorbitol-xylitol mixture: $C=17.16$ and $E_A=79$ (kJ/mol)]. The fitting uncertainties near $T_M$ are larger than those for below and above $T_M$. The base of the logarithm is 10.

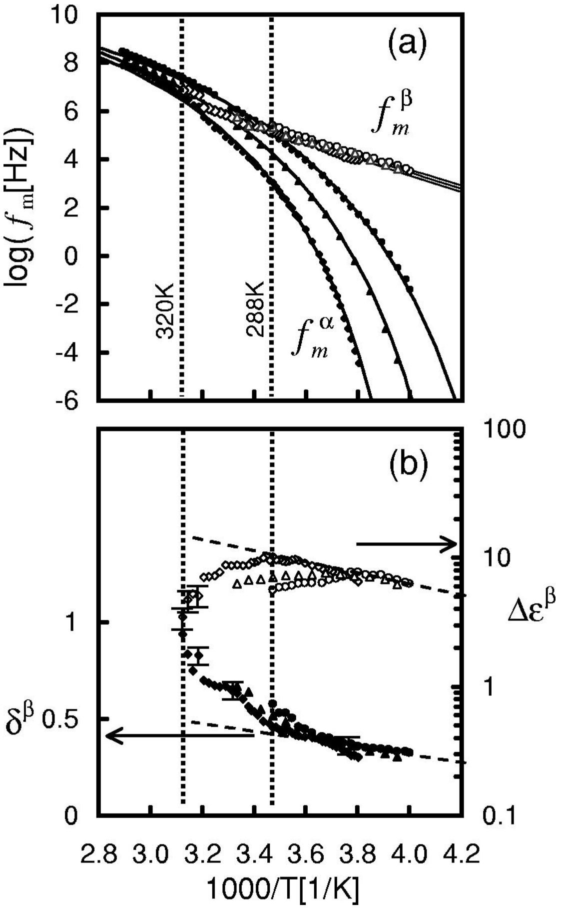

FIG. 4. Dotted lines represent $T_M$ of sorbitol (320 K) and xylitol (288 K), respectively. (a) Arrhenius diagram of sorbitol, xylitol, and mixture. Symbols are the same as those used in Fig. 3. (b) Temperature dependences of $\Delta\varepsilon^\beta$ and $\delta^\beta$ for sorbitol, xylitol, and the mixture. Open diamonds, open circles, and open triangles represent $\Delta\varepsilon^\beta$ for sorbitol, xylitol, and the mixture, respectively. Solid diamonds, solid circles, and solid triangles represent $\delta^\beta$ for sorbitol, xylitol, and the mixture, respectively. The base of the logarithm is 10.

dence and the behavior is quite similar to each other. Figure 3 shows the behavior of the $\beta$ processes in sorbitol, xylitol, and the mixture. The temperature dependences of $f_m^\beta$ for all the materials are described well by the solid lines obtained from Eq. (5). The values of parameter $C$ for all the materials are roughly 17. The values of the activation energy are $E_A=80$ (kJ/mol) for sorbitol, $E_A=78$ (kJ/mol) for xylitol, and $E_A=79$ (kJ/mol) for the mixture.

The values of the activation energy of the $\beta$ processes in sorbitol and xylitol are somewhat larger than those reported in a literature [29]. However, it should be noted that the values of the activation energy in this literature were obtained from the data below $T_g$. It is not very strange that there is difference in the activation energies below and above $T_g$. Actually, such a difference in sorbitol has been reported in Ref. [13].

As mentioned earlier, only one dielectric relaxation process for the $\alpha$ process is observed in the mixture. $f_m^\alpha$, $\Delta\varepsilon^\alpha$, and the $T_g^*$ of the mixture are intermediate value between those of sorbitol and xylitol. Namely, the mixture behaves like a pure material whose number of carbon is 5.5 in a molecule because these for sorbitol and xylitol are 6 and 5, respectively. However, the values of the shape parameters $\gamma^{\alpha}$ and $\delta^{\alpha}$ for sorbitol, xylitol, and the mixture are similar to each other. The values of $\gamma^{\alpha}$ and $\delta^{\alpha}$ for all the materials are 0.4 and 0.8 respectively. Therefore, it can be considered that the mixture has a large mean dynamical structure, which is directly connected to the $\alpha$ process. A considerable large number of molecules causes the origin of the $\alpha$ process even at temperatures right below $T_M$. If the $\alpha$ process is caused by orientational motion of a molecule, several processes in the mixture will be observed because $f_m^{\alpha}$ of sorbitol and xylitol at the same temperature are quite different. According to the idea of the cooperatively rearranging region (CRR) [4–6], the $\alpha$ process can be explained by the cooperative motion of some molecules. In this case, the relaxation time of the $\alpha$ process is the rate of the molecular motion cooperatively reorientating. The experimental results support the existence of the CRR.

In general, it would be expected that the mixed materials are microscopically heterogeneous and the values of the relaxation parameters of the mixed materials are different from those of pure constituents. As for aqueous solutions such as alcohol-water mixtures [36–38], the relaxation frequency and the relaxation strength of the $\alpha$ process are intermediate between those of pure constituents, and the distribution of the relaxation time is different from that of pure constituents. Therefore, the effect of mixing on the distribution of the relaxation time of usual liquids is different from that of supercooled liquids according to our study. It is considered that this difference comes from the difference in the size of CRR. The size of the CRR of usual liquids should be very small.

Figure 4(b) shows the temperature dependence of the relaxation strength of the $\beta$ process, $\Delta\varepsilon^{\beta}$, and the Cole-Cole shape parameter of the $\beta$ process, $\delta^{\beta}$, for sorbitol, xylitol, and the mixture. These relaxation parameters show anomalous behavior near $T_M$. However, except for near $T_M$, the values of $\Delta\varepsilon^{\beta}$ for sorbitol, xylitol, and the mixture are similar to each other and show the same temperature dependence where $\Delta\varepsilon^{\beta}$ increases with increasing temperature. On the other hand, the value and the behavior of $\delta^{\beta}$ for sorbitol, xylitol, and the mixture are also similar to each other. The values of $\delta^{\beta}$ increase with increasing temperature as well as $\Delta\varepsilon^{\beta}$. Thus, from the behavior of $f_m^{\beta}$, $\Delta\varepsilon^{\beta}$, and $\delta^{\beta}$, it is strongly suggested that the molecular origin of the $\beta$ processes in sorbitol, xylitol, and the mixture is essentially the same.

We have suggested a simply kinetic model as the origin of the $\beta$ process in sorbitol [23]. There are the hydrogen bonds among sorbitol molecules, which behave like water molecules bounded to sorbitol molecules. At lower temperatures, polyol molecules are orientationally correlated and the stable spaces exist among polyol molecules for the relaxation time of the $\alpha$ process. In the stable spaces, the hydrogen bonds among polyol molecules behave as water molecules bounded to polyol molecules. Since the relaxation time of the $\alpha$ process is much longer than the relaxation time of the $\beta$ process, the spaces among polyol molecules are stable during the dipolar relaxation of the waterlike structure produced by the hydrogen bonds among molecules. The dipolar relaxation can be considered as a thermally activated process with double minimum potential. Then, the $\beta$ process shows the Arrhenius-type temperature dependence. Since this story can be attributed to any polyols, it can be considered that the $\beta$ processes in all the polyols have similar behavior. However, there would be a strong correlation between the $\alpha$ and $\beta$ processes near $T_M$ and the behavior of the $\alpha$ process depends on the size of polyol molecule. Therefore, it seems that the appearance of the $\beta$ processes in polyols is different.

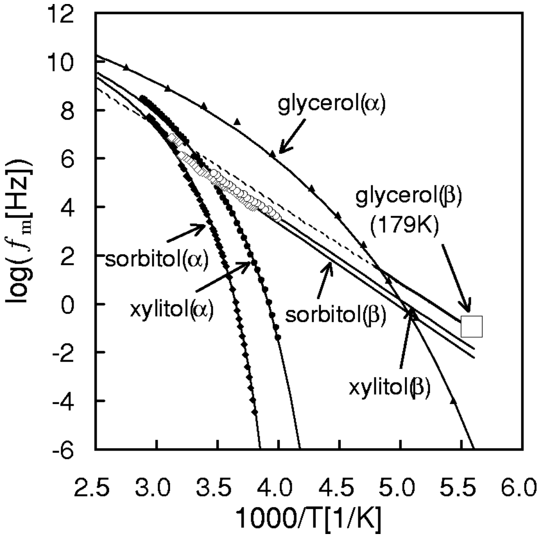

FIG. 5. Arrhenius diagram of sorbitol, xylitol, and glycerol. Solid diamonds, solid circles, and solid triangles represent $f_m^{\alpha}$ for sorbitol, xylitol, and glycerol, respectively. For glycerol, $f_m^{\alpha}$ are obtained from a report [18] and an open square is the secondary relaxation frequency at 179 K [19]. The VFT curve of glycerol was from a report [18]. Dashed and solid lines show the behavior of the $\beta$ process in glycerol estimated by us. The base of the logarithm is 10.

Based on above consideration about the relaxation processes in sorbitol and xylitol, we discuss the behavior of the relaxation process in glycerol. $T_m$ and $T_g^*$ of glycerol are 291 K and 190 K [39], respectively. The fragility index $m$ has been reported to be 53 [39]. Although glycerol belongs to a series of polyols, the $\beta$ process has not been clearly observed but the excess wing [17–19].

Figure 5 is the Arrhenius diagram of polyols including glycerol in addition to the materials being studied in this work. The plots for sorbitol and xylitol are from our measurements and those of the $\alpha$ process for glycerol from a report [18]. The dashed and solid lines in Fig. 4 show the behavior of the $\beta$ process in glycerol estimated by us. In Arrhenius function for the $\beta$ process in glycerol, the value of parameter $C$ was set about 17 same as that of sorbitol and xylitol. The value of the activation energy was estimated to be 74 (kJ/mol) by the linearly extrapolation from those of sorbitol, xylitol, and the mixture.

Schneider *et al.* performed isothermal complex permittivity measurements on glycerol at 179 K lasting up to five weeks and asserted that the secondary relaxation process de-

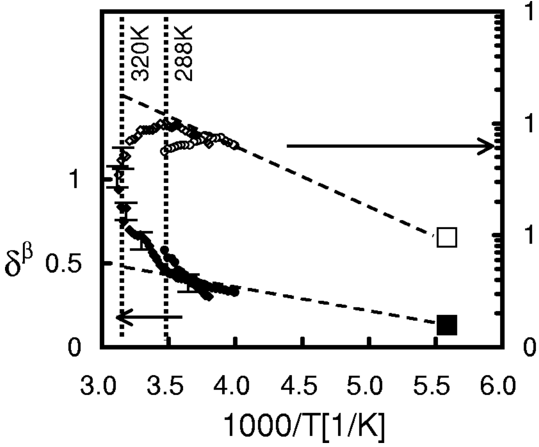

FIG. 6. $\Delta\varepsilon^\beta$ and $\delta^\beta$ for sorbitol, xylitol, and glycerol. Dotted lines represent $T_M$ of sorbitol (320 K) and xylitol (288 K), respectively. Open diamonds and open circles represent $\Delta\varepsilon^\beta$ for sorbitol and xylitol. Solid diamonds and solid circles represent $\delta^\beta$ for sorbitol and xylitol. Open and solid squares are $\Delta\varepsilon$ and $\delta$ of the secondary relaxation process in glycerol at 179 K, respectively [19].

scribed by Cole-Cole function was observed [19]. Their experimental value of the secondary relaxation frequency at 179 K is indicated in Fig. 4. In this figure, it is shown that our prediction for the secondary relaxation frequency of glycerol is in good agreement with the reported one.

Figure 6 shows the temperature dependence of $\Delta\varepsilon^\beta$ and $\delta^\beta$ for sorbitol and xylitol with the values of $\Delta\varepsilon$ and $\delta$ for those of the secondary relaxation process in glycerol at 179 K given by Schneider *et al.* [19]. The values of $\Delta\varepsilon$ and $\delta$ of the secondary relaxation process in glycerol agree with the lines naturally extrapolated using our experimental data for sorbitol and xylitol. This result implies that the secondary relaxation process in glycerol becomes broad and $\Delta\varepsilon$ decreases with decreasing temperature. It can be considered that this is a common feature of the $\beta$ process [15,21,41].

We expect that the $\beta$ process in glycerol can be observed at very lower temperatures. The $\beta$ process is appeared as the excess wing because the main part of the $\beta$ process is submerged in the dominating $\alpha$ process and the values of $\Delta\varepsilon^\beta$ are very small at lower temperatures. It is concluded that the excess wing is due to the high-frequency slope of the $\beta$ process as some experimentalists have been reported in their literatures [19,29,40,41].

Finally, we suggest that the $\beta$ processes in all the polyols have essentially the same molecular origin. Recently, Döß *et al.* have discussed on the difference between glycerol and sorbitol from the viewpoint of local mobility [29]. They claimed that the mobility of the intermolecular hydrogen bond is rather restricted compared to that of the molecular backbone for glycerol, while these are the same for sorbitol. However, this difference between glycerol and sorbitol shows up only below $T_g$. Actually, their data of the spin-lattice relaxation times indicate that there is no difference between glycerol and sorbitol above $T_g$. Our suggestion is consistent with this fact.

## IV. CONCLUSION

Complex permittivities of sorbitol, xylitol, and sorbitol-xylitol mixture in the supercooled liquid state were measured by means of broadband dielectric measurements. Since supercooled liquids are in the quasiequilibrium state, the behavior of all the relaxation parameters for the $\beta$ process can be compared among the polyols as well as those for the $\alpha$ process. The loci of the VFT functions of the $\alpha$ processes in sorbitol, xylitol, and the mixture are different corresponding to the difference in $T_g^*$. The relaxation parameters of the $\alpha$ process in sorbitol-xylitol mixture behave as if the mixture is a pure material, which consists of molecule whose size is between those of sorbitol and xylitol. This supports the existence of the CRR. On the other hand, the behavior of the $\beta$ processes in all the polyols including glycerol is similar. It can be considered that the $\beta$ processes in polyols have a common origin: the hydrogen bonds among molecules, which are strongly bounded to molecules and behave like bound water. Our consideration about the behavior of the $\alpha$ and $\beta$ processes supports that the excess wing in glycerol is due to the high-frequency slope of the $\beta$ process submerged in the $\alpha$ process. The $\beta$ process in glycerol, which has very small relaxation strength, would be observed at very low temperatures. It seems that the appearance of the $\beta$ processes in polyols is different since the behavior of the $\alpha$ processes depends on the size of molecule. However, the behavior and origin of the $\beta$ processes in polyols are the same.

[1] H. Vogel, Phys. Z. **22**, 645 (1921).
[2] G.S. Fulcher, J. Am. Ceram. Soc. **8**, 339 (1925).
[3] G. Tammann and W. Hesse, Z. Anorg. Allg. Chem. **156**, 245 (1926).
[4] G. Adam and J.H. Gibbs, J. Chem. Phys. **43**, 139 (1965).
[5] S. Matsuoka and X. Quan, Macromolecules **24**, 2770 (1991).
[6] K.L. Ngai, R.W. Rendell, and D.J. Plazek, J. Chem. Phys. **94**, 3018 (1991).
[7] W. Götze and L. Sjögren, Rep. Prog. Phys. **55**, 241 (1992).
[8] F. Garwe *et al.*, Macromolecules **29**, 247 (1996).
[9] K.L. Ngai, Solid State Phys. **9**, 121 (1979).
[10] K.Y. Tsang and K.L. Ngai, Phys. Rev. E **54**, R3067 (1996); **56**, R17 (1997).
[11] K.L. Ngai, J. Chem. Phys. **109**, 6982 (1998).
[12] G.P. Johari and M. Goldstein, J. Chem. Phys. **53**, 2372 (1970).
[13] H. Wagner and R. Richert, J. Phys. Chem. B **103**, 4071 (1999).
[14] J.Y. Cavaille, J. Perez, and G.P. Johari, Phys. Rev. B **39**, 2411 (1989).
[15] E. Donth, in *The Glass Transition*, edited by A. Zunger *et al.* (Springer, Berlin, 2001), p. 75.
[16] S. Kahle, K. Schröter, E. Hempel, and E. Donth, J. Chem. Phys. **111**, 6462 (1999).
[17] A. Kudlik *et al.*, J. Mol. Struct. **479**, 201 (1999).
[18] U. Schneider, P. Lunkenheimer, R. Brand, and A. Loidl, J. Non-Cryst. Solids **235–237**, 173 (1998).

[19] U. Schneider, R. Brand, P. Lunkenheimer, and A. Loidl, Phys. Rev. Lett. **84**, 5560 (2000).
[20] U. Schneider, P. Lunkenheimer, R. Brand, and A. Loidl, Phys. Rev. E **59**, 6924 (1999).
[21] R. Nozaki, D. Suzuki, S. Ozawa, and Y. Shiozaki, J. Non-Cryst. Solids **235–237**, 393 (1998).
[22] R. Nozaki, S. Ozawa, and Y. Shiozaki, in *Slow Dynamics in Complex Systems*, edited by M. Tokuyama and I. Oppenheim, AIP Conf. Proc. No. 469 (AIP, Melville, NY, 1999), p. 521.
[23] R. Nozaki, H. Zenitani, A. Minoguchi, and K. Kitai, J. Non-Cryst. Solids **307–310**, 349 (2002).
[24] A. Minoguchi and R. Nozaki, J. Non-Cryst. Solids **307–310**, 246 (2002).
[25] R. Richert, Europhys. Lett. **54**, 767 (2001).
[26] T. Fujima, H. Frusawa, K. Ito, and R. Hayakawa, Jpn. J. Appl. Phys., Part 2 **39**, L744 (2000).
[27] A. Faivre *et al.*, Eur. Phys. J. B **10**, 277 (1999).
[28] N.B. Olsen, J. Non-Cryst. Solids **235–237**, 399 (1998).
[29] A. Döß, M. Paluch, H. Sillescu, and G. Hinze, Phys. Rev. Lett. **88**, 095701 (2002).
[30] Riku A. Talja and Yrjö H. Roos, Thermochim. Acta **380**, 109 (2001).
[31] S. Havriliak and S. Negami, Polymer **8**, 161 (1967).
[32] K.S. Cole and R.H. Cole, J. Chem. Phys. **9**, 341 (1941).
[33] F. Stickel, E.W. Fischer, and R. Richert, J. Chem. Phys. **102**, 6251 (1995).
[34] F. Stickel, E.W. Fischer, and R. Richert, J. Chem. Phys. **104**, 2043 (1996).
[35] C. Hansen *et al.*, J. Chem. Phys. **107**, 1086 (1997).
[36] T. Sato, A. Chiba, and R. Nozaki, J. Chem. Phys. **112**, 2924 (2000).
[37] T. Sato, A. Chiba, and R. Nozaki, J. Chem. Phys. **113**, 9748 (2000).
[38] S. Sudo, N. Shinyashiki, Y. Kitsuki, and S. Yagihara, J. Phys. Chem. A **106**, 458 (2002).
[39] R. Böhmer, K.L. Ngai, C.A. Angell, and D.J. Plazek, J. Non-Cryst. Solids **99**, 4201 (1993).
[40] P. Lunkenheimer, R. Wehn, Th. Riegger, and A. Loidl, J. Non-Cryst. Solids **307–310**, 336 (2002).
[41] K.L. Ngai *et al.*, J. Chem. Phys. **115**, 1405 (2001).